Physica D 241 (2012) 115–124

Contents lists available at SciVerse ScienceDirect

Physica D

journal homepage: www.elsevier.com/locate/physd

On the validity of the variational approximation in discrete nonlinear Schrödinger equations

Christopher Chong [a,b], Dmitry E. Pelinovsky [a,c,*], Guido Schneider [a]

[a] Institut für Analysis, Dynamik und Modellierung, Universität Stuttgart, 70569 Stuttgart, Germany

[b] Department of Mathematics and Statistics, University of Massachusetts, Amherst, MA 01003-4515, USA

[c] Department of Mathematics, McMaster University, Hamilton ON, L8S 4K1, Canada

ARTICLE INFO

Article history:
Received 8 July 2011
Received in revised form
26 September 2011
Accepted 13 October 2011
Available online 19 October 2011
Communicated by J. Bronski

Keywords:
Discrete nonlinear Schrodinger equation
Variational approximation
Discrete solitons
Anti-continuum limit

ABSTRACT

The variational approximation is a well known tool to approximate localized states in nonlinear systems. In the context of a discrete nonlinear Schrödinger equation with a small coupling constant, we prove error estimates for the variational approximations of site-symmetric, bond-symmetric, and twisted discrete solitons. This is shown for various trial configurations, which become increasingly more accurate as more parameters are taken. It is also shown that the variational approximation yields the correct spectral stability result and controls the oscillatory dynamics of stable discrete solitons for long but finite time intervals.

1. Introduction

The discrete nonlinear Schrödinger (DNLS) equation is a relevant model for a wide range of applications including nonlinear optics (waveguide arrays), matter waves (Bose–Einstein condensates trapped in optical lattices) and molecular biology (modeling the DNA double strand) [1]. The existence of localized states, such as discrete solitons, prove particularly useful in such applications. A collection of results pertaining to existence, stability, and dynamics of localized states in the DNLS equation can be found in references [1,2].

The so-called variational approximation (VA) has long been used as a semi-analytical method to approximate localized states of nonlinear systems [3,4]. The method is based on the substitution of an ansatz (trial configuration of the wave field with a finite number of parameters) into the Lagrangian of the equation, and seeking critical points in the finite-dimensional subspace. Although this approach has been used for several decades, there are few rigorous results connecting the approximate solutions of the VA and true solutions of the nonlinear systems. In fact, the only work to this effect that the authors are aware of is due to Kaup and Vogel [5], where a quantitative measurement of the VA can be found by solving an associated linear nonhomogeneous equation. Although this approach can be applied to a broad range of problems, no rigorous estimates of the error of the variational approximation have been shown.

Heuristically, in the context of the DNLS equation, one would expect the VA to be more accurate for small coupling strength since the typical ansatz is based on an exponential cusp. As the coupling is increased and the continuum is approached, exact solutions become increasingly smooth (sech-like), and thus the VA becomes irrelevant. A number of recent works confirmed predictions of the variational method for existence and stability of lattice solitons in DNLS equations [6–9] by comparison with numerical solutions. It is the goal of this work to make this heuristic argument rigorous, thereby justifying the variational approximation in DNLS equations for the first time.

We consider a discrete nonlinear Schrödinger equation of the form,

$$i\dot{u}_n + |u_n|^2 u_n = -\epsilon(u_{n+1} - 2u_n + u_{n-1}), \quad n \in \mathbb{Z},\ t \in \mathbb{R}, \tag{1}$$

where $u_n(t)$ is the complex discrete wave field, n is the integer lattice coordinate, and real ϵ is the coupling strength between wave fields at the adjacent lattice sites.

Steady-state solutions have the form

$$u_n(t) = \psi_n e^{i(1-2\epsilon)t}, \tag{2}$$

where amplitudes ψ_n are time-independent. Although (2) is not a general steady-state solution of (1), a scaling of t, ψ_n, and ϵ can be used to recover a full family of steady-state solutions of (1) from

* Corresponding author at: Department of Mathematics, McMaster University, Hamilton ON, L8S 4K1, Canada.
E-mail address: dmpeli@math.mcmaster.ca (D.E. Pelinovsky).

0167-2789/$ – see front matter © 2011 Elsevier B.V. All rights reserved.
doi:10.1016/j.physd.2011.10.004

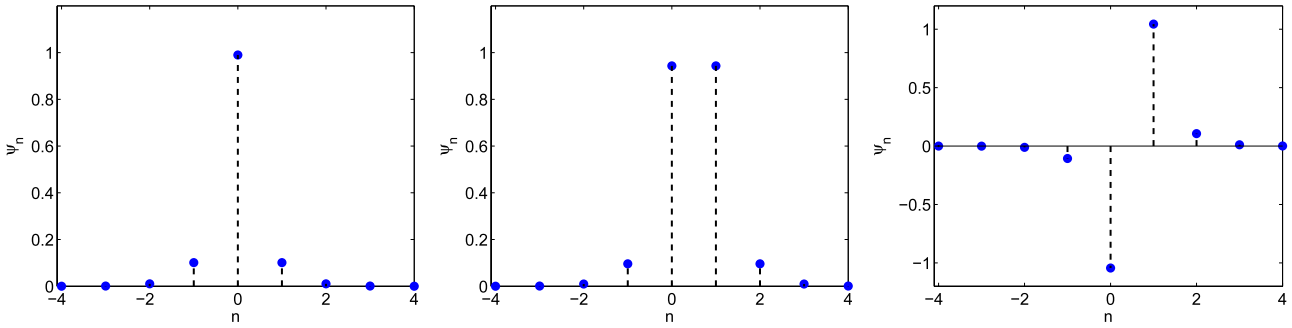

Fig. 1. Three examples of discrete solitons of the DNLS equation (3) for $\epsilon = 0.1$. Trial functions $\psi^{(1)}$ and $\psi^{(2)}$ approximate the site-symmetric soliton (left), function $\psi^{(3+)}$ corresponds to bond-symmetric solitons (middle), and function $\psi^{(3-)}$ captures the twisted soliton (right).

(2). Upon the substitution of (2) into the DNLS equation (1), we obtain the stationary equation,

$$(|\psi_n|^2 - 1)\psi_n = -\epsilon(\psi_{n-1} + \psi_{n+1}), \quad n \in \mathbb{Z}. \tag{3}$$

Existence and stability of spatially decaying solutions (called discrete solitons) of the DNLS equation is a well-studied subject [1,2]. In particular, it is well known that the soliton amplitudes ψ_n in one spatial dimension $n \in \mathbb{Z}$ are real-valued module to multiplication by $e^{i\theta}$ with $\theta \in \mathbb{R}$.

Spectral stability of discrete solitons is studied with the linearization ansatz,

$$u_n(t) = \left(\psi_n + (v_n + iw_n)e^{\lambda t} + (\bar{v}_n + i\bar{w}_n)e^{\bar{\lambda} t}\right) e^{i(1-2\epsilon)t}, \quad n \in \mathbb{Z},$$

which leads to the spectral problem,

$$\begin{cases} v_n - \epsilon(v_{n+1} + v_{n-1}) - 3\psi_n^2 v_n = -\lambda w_n, \\ w_n - \epsilon(w_{n+1} + w_{n-1}) - \psi_n^2 w_n = \lambda v_n, \end{cases} \quad n \in \mathbb{Z}. \tag{4}$$

We seek nonzero solutions of the linearized system in $l^2(\mathbb{Z}, \mathbb{C}^2)$. If there exists at least one such solution with $\mathrm{Re}(\lambda) > 0$, the discrete soliton is called unstable. Otherwise, it is called spectrally stable.

We consider a number of variational approximations of discrete solitons of the stationary equation (3). The first approximation is common in the application of the averaged Lagrangian method [10,11],

$$\psi_n^{(1)} = Ae^{-\eta|n|}, \quad n \in \mathbb{Z}, \tag{5}$$

where the parameters $A \in \mathbb{R}$ and $\eta \in \mathbb{R}_+$ are to be determined. This approximation describes the site-symmetric soliton of the DNLS equation (1) shown in Fig. 1 (left). A more accurate approximation for the site-symmetric soliton can be sought in the form,

$$\psi_n^{(2)} = \begin{cases} B & n = 0, \\ Ae^{-\eta(|n|-1)} & |n| \in \mathbb{N}, \end{cases} \tag{6}$$

which has an additional parameter $B \in \mathbb{R}$ to be determined. If $A = Be^{-\eta}$, then $\psi_n^{(2)}$ reduces to $\psi_n^{(1)}$. To consider solitons residing on two lattice sites, we can define

$$\psi_n^{(3)} = \begin{cases} B & n = 1, \\ Ae^{-\eta(n-2)} & n \geq 2, \end{cases} \tag{7}$$

and use symmetric and anti-symmetric reflections of $\psi_n^{(3)}$,

$$\psi_{1-n}^{(3\pm)} = \pm\psi_n^{(3\pm)}, \quad n \in \mathbb{N}, \tag{8}$$

where the parameters $A, B \in \mathbb{R}$, $\eta \in \mathbb{R}_+$ are to be determined. The symmetric reflection $\psi_n^{(3+)}$ corresponds to the bond-symmetric soliton of the DNLS equation (1) and the anti-symmetric reflection $\psi_n^{(3-)}$ describes the twisted soliton [12]. These two solitons are shown in Fig. 1 (middle) and (right) respectively.

The Lagrangian of the stationary DNLS equation (3) is

$$\mathcal{L}(\psi) = \sum_{n\in\mathbb{Z}} \left[\frac{1}{2}|\psi_n|^4 - |\psi_n|^2 + \epsilon(\bar{\psi}_n\psi_{n+1} + \psi_n\bar{\psi}_{n+1})\right]. \tag{9}$$

According to the variational principle, critical points of Lagrangian (9) correspond to solutions of the stationary DNLS equation (3). This motivates the averaged Lagrangian method, i.e. when a variational ansatz is substituted to the Lagrangian and parameters of the variational approximation are found from the Euler–Lagrange equations.

A more general variational ansatz can be used in the form,

$$\psi_n^{(K)} = Ae^{-\eta|n-s|}, \quad n \in \mathbb{Z}, \tag{10}$$

where the parameters $A \in \mathbb{R}$, $\eta \in \mathbb{R}_+$, and $s \in [0, 1]$ are to be determined. Ansatz (10) interpolates between the site-symmetric soliton for $s = 0$ and the bond-symmetric soliton for $s = \frac{1}{2}$. We will refer to this ansatz as Kaup's approximation due to the pioneer work in [8]. Kaup's approximation was found to be fairly accurate in the stationary case [6,8,9] and in the approximation of spectral stability [6] using a time-dependent variant of the ansatz (10).

Since the exponential decay rate of discrete solitons follow from the linear theory of difference equations, we will fix the parameter η uniquely from the equation,

$$1 = \epsilon(e^{\eta} + e^{-\eta}) \Rightarrow \eta = \mathrm{arccosh}\left(\frac{1}{2\epsilon}\right), \tag{11}$$

which yields the asymptotic expansion,

$$e^{-\eta} = \epsilon + \epsilon^3 + \mathcal{O}(\epsilon^5) \quad \text{as } \epsilon \to 0. \tag{12}$$

We have chosen to fix η in this way to make the analysis more tractable. This is in contrast to the ansatz that Kaup considered in [8], where η was time dependent.

In what follows, we derive values of the remaining parameters of the variational approximations (5)–(8) using the averaged Lagrangian method. We show that the error term of the variational approximations can be controlled by powers of ϵ and the trial functions with more parameters are more accurate as their errors converge to zero with a higher exponent in the power of ϵ.

Using Kaup's approximation (10) for the stationary equation (3), we are able to recover both the site-symmetric and bond-symmetric solitons in Fig. 1 (left and middle). The error of this approximation is the same as for the one-parameter trial function (5). We also modify Kaup's approximation to study the time-dependent evolution of the stable site-symmetric soliton in the DNLS equation (1). We recover correct predictions of spectral stability of site-symmetric solitons and spectral instability of bond-symmetric solitons. In addition, we are able to control the error of the variational approximation for bounded oscillations of a discrete soliton near a stable equilibrium state for long but finite time intervals.

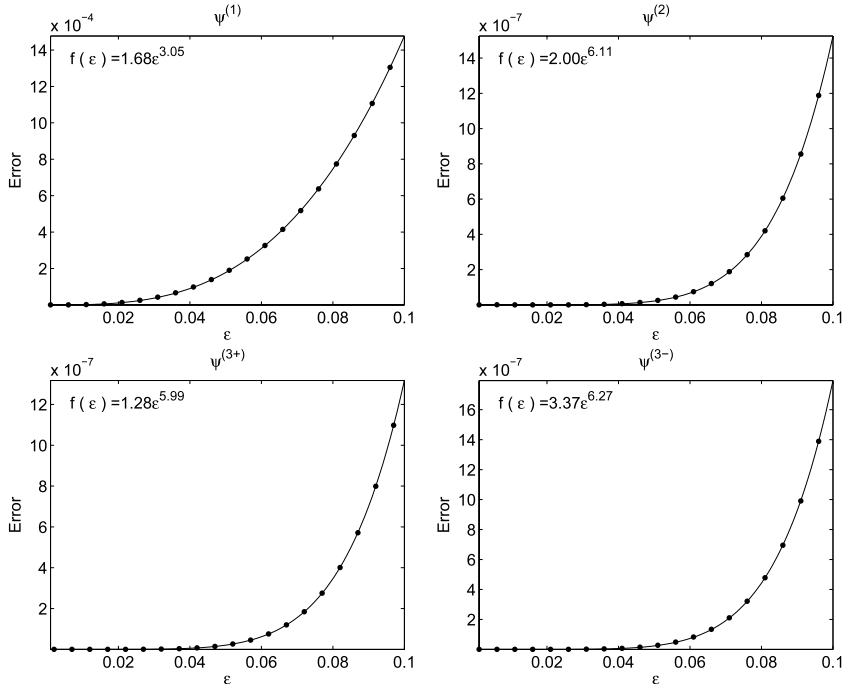

Fig. 2. Error, measured in the l^2 norm, between the variational and numerical solutions of the stationary equation (3) for various values of the coupling strength ϵ. The solid line shows the best power fit of the form $f(\epsilon) = C\epsilon^p$, where $C > 0$ and $p > 0$. The top row corresponds to the site-symmetric ansatz $\psi^{(1)}$ (left) and $\psi^{(2)}$ (right). The bottom row shows the two-site ansatz $\psi^{(3+)}$ (left) and $\psi^{(3-)}$ (right).

The article is organized as follows. Section 2 provides the proof of validity of the variational approximation given by trial functions (5)–(8). Kaup's approximation (10) in the stationary case is justified in Section 3. The time-dependent solutions modeled by Kaup's approximations are studied in Section 4. Section 5 concludes the article.

2. Justification of the stationary variational approximations

We define the residual of the stationary DNLS equation (3) as

$$R_n(\psi) = (|\psi_n|^2 - 1)\psi_n + \epsilon(\psi_{n-1} + \psi_{n+1}). \tag{13}$$

The residual is used to measure the accuracy of the variational approximation, in accordance with the following lemma.

Lemma 1. *Let ψ_* be an approximate solution of the stationary DNLS equation (3) such that*

$$\|R(\psi_*)\|_{l^2} = \mathcal{O}(\epsilon^p) \quad \text{as } \epsilon \to 0 \tag{14}$$

for some $p > 0$ and there is a finite set $S \subset \mathbb{Z}$ and a binary set $\{\sigma_n\}_{n\in S}$ with $\sigma_n \in \{+1, -1\}$ such that

$$\lim_{\epsilon\to 0} \left\| \psi_* - \sum_{n\in S} \sigma_n e_n \right\|_{l^2} = 0, \tag{15}$$

where e_n is the unit vector on site $n \in \mathbb{Z}$ in $l^2(\mathbb{Z})$. Then, there are $\epsilon_0 > 0, C > 0$, and a unique solution of the stationary DNLS equation with $\epsilon \in (0, \epsilon_0)$ such that

$$\|\psi - \psi_*\|_{l^2} \le C\epsilon^p.$$

Proof. We substitute $\psi = \psi_* + \varphi$ to (3) and obtain,

$$L\varphi = R(\psi_*) + N(\varphi), \tag{16}$$

where $R(\psi_*) \in l^2(\mathbb{R})$ is the residual (13), $L : l^2(\mathbb{Z}) \to l^2(\mathbb{Z})$ is a bounded operator given by

$$(L\varphi)_n = (1 - 3\psi_{*n}^2)\varphi_n - \epsilon(\varphi_{n+1} + \varphi_{n-1}),$$

and $N(\varphi) : l^2(\mathbb{Z}) \to l^2(\mathbb{Z})$ is a Lipschitz map in a ball $B_\delta \subset l^2(\mathbb{Z})$ of any radius $\delta > 0$ centered at 0 given by $N_n(\varphi) = 3\psi_{*n}\varphi_n^2 + \varphi_n^3$. In particular, there are constants $C_\delta, D_\delta > 0$, which depend on $\delta > 0$, such that for all $\varphi_1, \varphi_2 \in B_\delta$,

$$\|N(\varphi)\|_{l^2} \le C_\delta \|\varphi\|_{l^2}^2$$

and

$$\|N(\varphi_1) - N(\varphi_2)\|_{l^2} \le D_\delta(\|\varphi_1\|_{l^2} + \|\varphi_2\|_{l^2})\|\varphi_1 - \varphi_2\|_{l^2}.$$

Condition (15) implies that the spectrum of L at $\epsilon = 0$ includes only points 1 and -2. Since the spectrum at $\epsilon = 0$ is bounded away from zero, the operator L is invertible for any small $\epsilon \in \mathbb{R}$. Therefore, we can write (16) as

$$\varphi = A(\varphi) := L^{-1}R(\psi_*) + L^{-1}N(\varphi). \tag{17}$$

Condition (14) implies that the residual term is small so that the operator $A : B_\delta \to B_\delta$ is a contraction for some $\delta = \mathcal{O}(\epsilon^p)$. The result of the lemma follows by the Banach Fixed-Point Theorem. □

Here we will use Lemma 1 to justify the variational approximations (5)–(8) for the stationary DNLS equation (3) with small $\epsilon > 0$. The accuracy of the variational approximations in powers of ϵ is illustrated in Fig. 2, where we plot the error between the variational and numerical solutions of the stationary DNLS equation (3).

2.1. Approximation based on ansatz $\psi^{(1)}$

The substitution of the ansatz (5) into the Lagrangian (9) and the calculation of the ensuing sums yields the effective Lagrangian,

$$\begin{aligned} L(A) \equiv \mathcal{L}(\psi^{(1)}) &= \frac{1}{2}A^4 \coth(2\eta) - A^2 \coth(\eta) \\ &\quad + 2\epsilon A^2 (\coth(\eta)\cosh(\eta) - \sinh(\eta)) \\ &= \frac{1}{2}A^4 \coth(2\eta) - A^2\left(1 - 2\epsilon e^{-\eta}\right), \end{aligned} \tag{18}$$

where Eq. (11) has been used. Variation of A yields either $A = 0$ (zero solution) or

$$A^2 = \left(1 - 2\epsilon e^{-\eta}\right)\tanh(2\eta) = 1 - 2\epsilon^2 + \mathcal{O}(\epsilon^4) \quad \text{as } \epsilon \to 0. \tag{19}$$

On the other hand, the residual (13) evaluated at the ansatz (5) is given by

$$R_n(\psi^{(1)}) = \begin{cases} A(A^2 - 1 + 2\epsilon e^{-\eta}), & n = 0, \\ A^3 e^{-3\eta|n|}, & |n| \in \mathbb{N}. \end{cases}$$

If A^2 is defined by (19), then

$$R_0(\psi^{(1)}) = A(1 - 2\epsilon e^{-\eta})(\tanh(2\eta) - 1) = \mathcal{O}(\epsilon^4)$$

and

$$R_n(\psi^{(1)}) = A^3 e^{-3\eta|n|} = \mathcal{O}(\epsilon^{3|n|}), \quad |n| \in \mathbb{N},$$

so that $\|R(\psi^{(1)})\|_{l^2} = \mathcal{O}(\epsilon^3)$ as $\epsilon \to 0$. Lemma 1 yields the following statement.

Proposition 2. *Let η and A by given by (11) and (19), respectively. Then there exist $\epsilon_0, C > 0$ such that for all $\epsilon \in (0, \epsilon_0)$, the stationary DNLS equation (3) admits solutions $\psi \in l^2(\mathbb{Z})$ satisfying*

$$\|\psi - \psi^{(1)}\|_{l^2} \le C\epsilon^3.$$

The result of Proposition 2 is illustrated in Fig. 2 (top left).

2.2. Approximation based on ansatz $\psi^{(2)}$

The substitution of the ansatz (6) into the Lagrangian (9) and the calculation of the ensuing sums using Eq. (11) yields the effective Lagrangian,

$$L(A, B) \equiv \mathcal{L}(\psi^{(2)}) = \frac{A^4}{1 - e^{-4\eta}} - 2A^2(1 - \epsilon e^{-\eta}) + \frac{1}{2}B^4 - B^2 + 4\epsilon AB. \tag{20}$$

Variation in A and B yield respectively,

$$\frac{A^3}{1 - e^{-4\eta}} - A(1 - \epsilon e^{-\eta}) + \epsilon B = 0. \tag{21}$$

and

$$(B^2 - 1)B + 2\epsilon A = 0. \tag{22}$$

If we are looking for an approximation of the site-symmetric soliton, we are interested in the solution of (21) and (22) satisfying the asymptotic expansion,

$$B = 1 - \epsilon^2 + \mathcal{O}(\epsilon^4), \qquad A = \epsilon + \mathcal{O}(\epsilon^3) \quad \text{as } \epsilon \to 0. \tag{23}$$

On the other hand, the residual (13) evaluated at the ansatz (6) is given by

$$R_n(\psi^{(2)}) = \begin{cases} (B^2 - 1)B + 2\epsilon A, & n = 0, \\ (A^2 - 1 + \epsilon e^{-\eta})A + \epsilon B, & n = \pm 1, \\ A^3 e^{-3\eta|n-1|}, & |n| \ge 2. \end{cases}$$

If A and B are defined by (21) and (22) with the asymptotic expansion (23), then

$$R_0(\psi^{(2)}) = 0, \qquad R_{\pm 1}(\psi^{(2)}) = -\frac{A^3 e^{-4\eta}}{1 - e^{-4\eta}} = \mathcal{O}(\epsilon^7)$$

and

$$R_n(\psi^{(2)}) = A^3 e^{-3\eta|n-1|} = \mathcal{O}(\epsilon^{3|n|}), \quad |n| \ge 2,$$

so that $\|R(\psi^{(2)})\|_{l^2} = \mathcal{O}(\epsilon^6)$ as $\epsilon \to 0$. Lemma 1 yields the following statement.

Proposition 3. *Let η, A, and B be given by (11), (21) and (22), respectively, and (A, B) satisfy the asymptotic expansion (23). Then there exist $\epsilon_0, C > 0$ such that for all $\epsilon \in (0, \epsilon_0)$, the stationary DNLS equation (3) admits solutions $\psi \in l^2(\mathbb{Z})$ satisfying*

$$\|\psi - \psi^{(2)}\|_{l^2} \le C\epsilon^6.$$

The result of Proposition 3 is illustrated in Fig. 2 (top right).

2.3. Approximation based on ansatz $\psi^{(3\pm)}$

The substitution of the ansatz (7) and (8) into the Lagrangian (9) and the calculation of the ensuing sums using Eq. (11) yields the effective Lagrangian,

$$L(A, B) \equiv \mathcal{L}(\psi^{(3\pm)}) = \frac{A^4}{1 - e^{-4\eta}} - 2A^2(1 - \epsilon e^{-\eta}) + B^4 - 2B^2(1 \mp \epsilon) + 4\epsilon AB. \tag{24}$$

Variation in A and B yield,

$$\frac{A^3}{1 - e^{-4\eta}} - A(1 - \epsilon e^{-\eta}) + \epsilon B = 0. \tag{25}$$

and

$$(B^2 - 1)B + \epsilon A \pm \epsilon B = 0. \tag{26}$$

Approximations of the bond-symmetric soliton and the twisted soliton relies on the asymptotic solution of the system (25) and (26) given by

$$B = 1 \mp \frac{\epsilon}{2} + \mathcal{O}(\epsilon^2), \qquad A = \epsilon + \mathcal{O}(\epsilon^2) \quad \text{as } \epsilon \to 0. \tag{27}$$

The residual (13) evaluated at the ansatz (7) and (8) is given by

$$R_n(\psi^{(3\pm)}) = \begin{cases} (B^2 - 1)B + \epsilon A \pm \epsilon B, & n = 1, \\ (A^2 - 1 + \epsilon e^{-\eta})A + \epsilon B, & n = 2, \\ A^3 e^{-3\eta|n-2|}, & |n| \ge 3, \end{cases}$$

with the obvious reflection to $n \le 0$. If A and B are defined by (25) and (26) with the asymptotic expansion (27), then

$$R_1(\psi^{(3\pm)}) = 0, \qquad R_2(\psi^{(3\pm)}) = -\frac{A^3 e^{-4\eta}}{1 - e^{-4\eta}} = \mathcal{O}(\epsilon^7)$$

and

$$R_n(\psi^{(3\pm)}) = A^3 e^{-3\eta|n-2|} = \mathcal{O}(\epsilon^{3(|n|-1)}), \quad n \ge 3,$$

so that $\|R(\psi^{(3\pm)})\|_{l^2} = \mathcal{O}(\epsilon^6)$ as $\epsilon \to 0$. Lemma 1 yields the following statement.

Proposition 4. *Let η, A, and B be given by (11), (25) and (26), respectively, and (A, B) satisfy the asymptotic expansion (27). Then there exist $\epsilon_0, C > 0$ such that for all $\epsilon \in (0, \epsilon_0)$, the stationary DNLS equation (3) admits solutions $\psi \in l^2(\mathbb{Z})$ satisfying*

$$\|\psi - \psi^{(3\pm)}\|_{l^2} \le C\epsilon^6.$$

The result of Proposition 4 is illustrated in Fig. 2 (bottom left and right).

3. Kaup's approximation in the stationary case

Here we will justify Kaup's approximation (10) for solutions of the stationary DNLS equation (3). The substitution of (10) into the Lagrangian (9) and the calculation of the ensuing sums yields the effective Lagrangian,

$$L(A, \chi) \equiv \mathcal{L}(\psi^{(K)}) = \frac{1}{2}A^4 \frac{\cosh(2\eta\chi)}{\sinh(2\eta)} - 2\epsilon A^2(\cosh(\eta\chi) - e^{-\eta}), \tag{28}$$

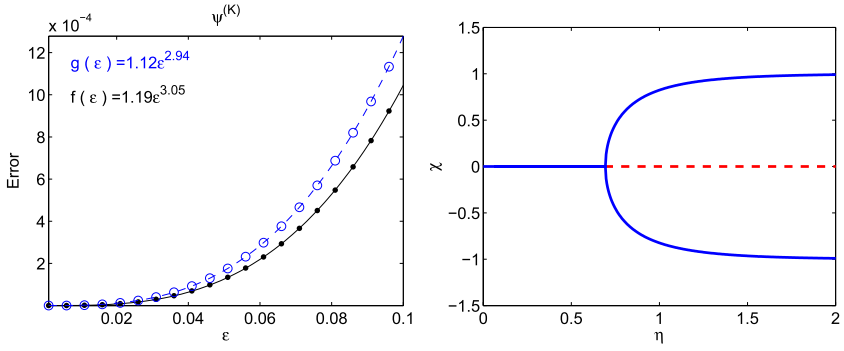

Fig. 3. Left: error, measured in the l^2 norm, between the variational and numerical solutions of the stationary equation (3). The circles correspond to $\psi^{(K)}$ with $\chi = 0$ (i.e. bond-symmetric soliton) and the dashed line shows the best power fit $g(\epsilon) = 1.12\epsilon^{2.94}$. The solid circles correspond to $\chi \approx -1$ (i.e. site-symmetric soliton) and the solid line shows the best power fit $f(\epsilon) = 1.19\epsilon^{3.05}$. Right: solutions of the transcendental equation (32) in the (η, χ) plane (solid lines) and the $\chi = 0$ solution. Both curves extend indefinitely to the right.

where $\chi = 2s - 1$. We have assumed here that $s \in [0, 1]$, hence $\chi \in [-1, 1]$. If $s = 0$ ($\chi = -1$), we recover the previous result (18). However, the difference is now that two equations follow from the effective Lagrangian (28) after variations with respect to A and χ. Assuming that $A \neq 0$, variations in χ show that

$$\text{either } \chi = 0 \quad \text{or} \quad A^2 = \epsilon \frac{\sinh(2\eta)}{\cosh(\eta\chi)}. \tag{29}$$

Variation in A yields

$$A^2 = 2\epsilon \frac{\sinh(2\eta)}{\cosh(2\eta\chi)} \left(\cosh(\eta\chi) - e^{-\eta}\right). \tag{30}$$

If $\chi = 0$ $\left(s = \frac{1}{2}\right)$, we obtain uniquely

$$A^2 = 2\epsilon \sinh(2\eta)(1 - e^{-\eta}) \Rightarrow A^2 e^{-\eta} = 1 - \epsilon - \epsilon^2 + \mathcal{O}(\epsilon^4). \tag{31}$$

This is the variational approximation of the bond-symmetric soliton shown in Fig. 1 (middle).

If $\chi \neq 0$, we can eliminate A^2 from the system (29) and (30) and find an equation for χ, which is reduced to the form,

$$e^{\eta(\chi-1)} + e^{-\eta(\chi+1)} = 1. \tag{32}$$

Using Eq. (11), we find uniquely for $\chi \approx -1$,

$$\eta(\chi + 1) = \epsilon^2 + \mathcal{O}(\epsilon^4)$$
$$\Rightarrow A^2 = 2\epsilon e^{-\eta} \sinh(2\eta) = 1 - \epsilon^2 + \mathcal{O}(\epsilon^4). \tag{33}$$

This is the variational approximation of the site-symmetric soliton shown in Fig. 1 (left).

Now we shall justify these approximations for small $\epsilon > 0$. The residual (13) evaluated at the ansatz (10) is given by

$$R_n(\psi^{(K)}) = \begin{cases} A^3 e^{-3\eta s} - A e^{-\eta s} + 2\epsilon A e^{-\eta} \cosh(\eta s), & n = 0, \\ A^3 e^{-3\eta(1-s)} - A e^{-\eta(1-s)} \\ \quad + 2\epsilon A e^{-\eta} \cosh(\eta(1-s)), & n = 1, \\ A^3 e^{-3\eta|n-s|}, & n \geq 2,\ n \leq -1. \end{cases}$$

If $\chi = 0$ $\left(s = \frac{1}{2}\right)$ and A is defined by (31), then we have

$$\begin{aligned} R_0(\psi^{(K)}) &= R_1(\psi^{(K)}) = A e^{-\eta/2} \left(A^2 e^{-\eta} - 1 + \epsilon + \epsilon e^{-\eta}\right) \\ &= -\epsilon A e^{-\eta/2} e^{-3\eta}(1 - e^{-\eta}) = \mathcal{O}(\epsilon^4) \end{aligned}$$

and

$$\begin{aligned} R_n(\psi^{(K)}) &= R_{-n+1}(\psi^{(K)}) = e^{-3\eta(n-1)} \left(A e^{-\eta/2}\right)^3 \\ &= \mathcal{O}(\epsilon^{3(n-1)}), \quad n \geq 2. \end{aligned}$$

If $\chi \approx -1$ is defined by (32) and A is defined by (33), then we have

$$\begin{aligned} R_0(\psi^{(K)}) &= A e^{-\eta(1+\chi)/2} \left(A^2 e^{-\eta(1+\chi)} - 1 + \epsilon e^{\eta\chi} + \epsilon e^{-\eta}\right) \\ &= -\epsilon A e^{-\eta(1+\chi)/2} e^{-4\eta-\eta\chi} = \mathcal{O}(\epsilon^4), \\ R_1(\psi^{(K)}) &= A e^{-\eta(1-\chi)/2} \left(A^2 e^{-\eta(1-\chi)} - 1 + \epsilon e^{-\eta\chi} + \epsilon e^{-\eta}\right) \\ &= -\epsilon A e^{-\eta(1-\chi)/2} e^{-4\eta+\eta\chi} = \mathcal{O}(\epsilon^7), \end{aligned}$$

$$R_{-1}(\psi^{(K)}) = e^{-3\eta} A^3 e^{-3\eta(\chi+1)/2} = \mathcal{O}(\epsilon^3).$$

and

$$R_{\pm n}(\psi^{(K)}) = e^{-3\eta|n|} A^3 e^{\pm 3\eta(\chi+1)/2} = \mathcal{O}(\epsilon^{3|n|}), \quad n \geq 2.$$

Since $\|R(\psi^{(K)})\|_{l^2} = \mathcal{O}(\epsilon^3)$ as $\epsilon \to 0$ in both cases, Lemma 1 yields the following statement.

Proposition 5. *Let η be given by (11) and let $\chi = 0$ and A be given by (31) or let χ and A be given by (32) and (33). Then there exist ϵ_0, $C > 0$ such that for all $\epsilon \in (0, \epsilon_0)$, the stationary DNLS equation (3) admits solutions $\psi \in l^2(\mathbb{Z})$ satisfying*

$$\|\psi - \psi^{(K)}\|_{l^2} \leq C\epsilon^3.$$

The result of Proposition 5 is illustrated in the left panel of Fig. 3 for both bond-symmetric ($\chi = 0$) and site-symmetric ($\chi \approx -1$) solitons. The right panel of Fig. 3 shows solutions of the transcendental equation (32). As η increases in the limit $\epsilon \to 0$, χ approaches ± 1 which corresponds to an exact site-symmetric soliton.

As first shown by Kaup in [8], the variational approximation falsely predicts that the bond- and site-symmetric solitons coalesce, which for our choice of ansatz occurs at $\eta \approx 0.69$($\epsilon \approx 0.40$). In [8], Kaup allowed η to be time dependent, and obviously obtained a different value for the coalescence point. Proposition 5 shows, however, that the false coalescence is not observed in the limit of small coupling constant ϵ.

4. Kaup's approximation in the time-dependent case

We shall now consider Kaup's approximation in the time-dependent DNLS equation, which we take in the form,

$$i\dot{u}_n + \epsilon(u_{n+1} + u_{n-1}) = (1 - |u_n|^2)u_n, \quad n \in \mathbb{Z},\ t \in \mathbb{R}. \tag{34}$$

Steady-state solitons become now time-independent solutions of the DNLS equation (34). The Lagrangian of the DNLS equation (34) is

$$\begin{aligned} \mathcal{L}(u) = \frac{i}{2} \sum_{n\in\mathbb{Z}} \left(\bar{u}_n \dot{u}_n - u_n \dot{\bar{u}}_n\right) + \frac{1}{2} \sum_{n\in\mathbb{Z}} |u_n|^4 \\ - \sum_{n\in\mathbb{Z}} |u_n|^2 + \epsilon \sum_{n\in\mathbb{Z}} (\bar{u}_n u_{n+1} + u_n \bar{u}_{n+1}). \end{aligned} \tag{35}$$

We shall consider a time-dependent trial function that generalizes the Kaup's approximation (10). A six-parameter trial function was used in our previous work [6]. It was shown that two parameters can be eliminated by using the conserved quantity and the cyclic variable. The remaining four-dimensional system obtained from the Euler–Lagrange equations was found to be qualitatively accurate in the prediction of stability and instability of discrete solitons in the cubic–quintic DNLS equation. In contrast to this earlier work, we shall herein consider a simplified four-parameter trial function in the form,

$$u_n^{(K)}(t) = Ae^{i\alpha+i\beta(n-s)-\eta|n-s|}, \quad n \in \mathbb{Z}, \tag{36}$$

where (A, α, β, s) are functions of time and η is uniquely determined as a function of $\epsilon > 0$ by the transcendental equation (11). Because of the symmetry of discrete translations on sites $n \in \mathbb{Z}$, for each $s \in (0, 1)$ we can introduce the variable $\chi = 2s - 1 \in (-1, 1)$ and extend this variable for other values of $s \in \mathbb{R}$ as a 2-periodic function with jumps at $\chi = \pm 1$. After the elimination of two parameters using conserved quantities, we will reduce the Euler–Lagrange equations to a planar system for parameters (β, χ), which accurately predicts stability of site-symmetric ($\chi = \chi_0 \approx -1$) solitons and instability of bond-symmetric ($\chi = 0$) solitons.

After substitution of (36) into (35), we obtain the effective Lagrangian,

$$\begin{aligned} L(A, \alpha, \beta, \chi) \equiv \mathcal{L}(u^{(K)}) &= -A^2\left(\dot{\alpha} - \frac{1}{2}\beta\dot{\chi}\right) S_0(\eta, \chi) \\ &\quad - A^2\dot{\beta}S_1(\eta, \chi) - A^2 S_0(\eta, \chi) + \frac{1}{2}A^4 S_0(2\eta, \chi) \\ &\quad + 2\epsilon A^2\cos(\beta)e^{-\eta}(1 + S_0(\eta, \chi)), \end{aligned} \tag{37}$$

where $\chi = 2s - 1 \in (-1, 1)$,

$$S_0(\eta, \chi) = \frac{\cosh(\eta\chi)}{\sinh(\eta)},$$

$$S_1(\eta, \chi) = \frac{1}{2}S_0(\eta, \chi)\left(\frac{\tanh(\eta\chi)}{\tanh(\eta)} - \chi\right).$$

We note that the effective Lagrangian (37) coincides with the one obtained in [6] subject to a sign misprint in S_1.

Variation of L in the cyclic variable α yields the conserved quantity,

$$A^2 S_0(\eta, \chi) = M = \text{ const} \Rightarrow A^2 = \frac{M\sinh(\eta)}{\cosh(\eta\chi)}. \tag{38}$$

Variation of L in the variable A defines the rate of change of α,

$$\frac{d\alpha}{dt} = \frac{1}{2}\beta\frac{d\chi}{dt} - \frac{S_1(\eta, \chi)}{S_0(\eta, \chi)}\frac{d\beta}{dt} + H(\beta, \chi), \tag{39}$$

where

$$\begin{aligned} H(\beta, \chi) &:= A^2\frac{\cosh(2\eta\chi)\sinh(\eta)}{\sinh(2\eta)\cosh(\eta\chi)} - 1 \\ &\quad + 2\epsilon\cos(\beta)e^{-\eta}\left(1 + \frac{\sinh(\eta)}{\cosh(\eta\chi)}\right). \end{aligned} \tag{40}$$

Note that equation $H(0, \chi) = 0$ recovers the stationary equation (30) with the help of Eq. (11).

After A and α are eliminated by Eqs. (38) and (39), we can close the system of Euler–Lagrange equations in β and χ as a planar system in the form

$$\frac{d\beta}{dt} = F(\beta, \chi), \qquad \frac{d\chi}{dt} = G(\beta, \chi). \tag{41}$$

Lengthy but straightforward computations yield the explicit expressions for the vector fields,

$$F(\beta, \chi) = \frac{\sinh^2(\eta)\sinh(\eta\chi)}{\cosh^2(\eta)\cosh(\eta\chi)}\left(M - 2\cos(\beta)e^{-\eta}\cosh(\eta\chi)\right),$$

$$G(\beta, \chi) = \frac{4\epsilon e^{-\eta}\sinh(\eta)\cosh(\eta\chi)}{\eta\cosh(\eta)}(\sinh(\eta) + \cosh(\eta\chi))\sin(\beta),$$

where M is the conserved quantity given by (38). The planar dynamical system (41) admits the conserved quantity,

$$\begin{aligned} E(\beta, \chi) &= -\frac{M\sinh(\eta)}{\cosh^2(\eta\chi)} \\ &\quad + 4e^{-\eta}\frac{\sinh(\eta) + \cosh(\eta\chi)}{\cosh(\eta\chi)}\cos(\beta) = E, \end{aligned} \tag{42}$$

which allows to plot the trajectories on the phase plane (β, χ) as the level set of functions $E = E(\beta, \chi)$. Fig. 4 shows the phase plane for two values of M and some particular numerical solutions of the planar system (41).

Let us study critical points of the planar system (41) in correspondence with the results of Section 3. First, we see that $(\beta, \chi) = (0, 0)$ is a critical point for any $M > 0$. Kaup's approximation (10) is recovered if $\alpha = \beta = 0$, which implies that

$$\begin{aligned} H(0, \chi) &= M\frac{\cosh(2\eta\chi)\sinh^2(\eta)}{\sinh(2\eta)\cosh^2(\eta\chi)} \\ &\quad - 2\epsilon\sinh(\eta) + 2\epsilon e^{-\eta}\frac{\sinh(\eta)}{\cosh(\eta\chi)} = 0. \end{aligned}$$

For the critical point $(\beta, \chi) = (0, 0)$, this equation yields,

$$M = 2(1 - e^{-\eta}), \tag{43}$$

which corresponds to the stationary equation (31), which explains the choice of $M = 1.79$ in Fig. 4 (right).

On the other hand, the planar system (41) has another critical point $(\beta, \chi) = (0, \chi_0)$ with $\chi_0 \neq 0$ if M is sufficiently large. If M is given by

$$M = 2\epsilon\cosh(\eta\chi_0)(1 + e^{-2\eta}), \tag{44}$$

then equation $H(0, \chi_0) = 0$ yields

$$e^{\eta(\chi_0 - 1)} + e^{-\eta(\chi_0 + 1)} = 1, \tag{45}$$

which is nothing but the stationary equation (32). Note that Eqs. (11) and (45) give

$$\begin{aligned} M &= 2\epsilon\cosh(\eta\chi_0)(1 + e^{-2\eta}) = 4\epsilon e^{-\eta}\cosh(\eta\chi_0)\cosh(\eta) \\ &= 2e^{-\eta}\cosh(\eta\chi_0) = 1, \end{aligned}$$

which explains the choice of $M = 1$ in Fig. 4 (left).

We shall now consider two results concerning the time-dependent evolution of the variational approximation (36). First, we recover the stability results for the site-symmetric and bond-symmetric discrete solitons from the planar system (41). Second, we control the error of the variational approximation for oscillations near the stable center point on long but finite time intervals.

4.1. Spectral stability

To check stability of critical points of the planar system (41), we linearize the system for small perturbations. Near the critical point $(0, 0)$, we find the perturbation equation $\ddot{\chi} = \lambda^2\chi$ with

$$\lambda^2 = \frac{4\epsilon e^{-\eta}\sinh^3(\eta)}{\cosh^3(\eta)}(1 + \sinh(\eta))(M - 2e^{-\eta}).$$

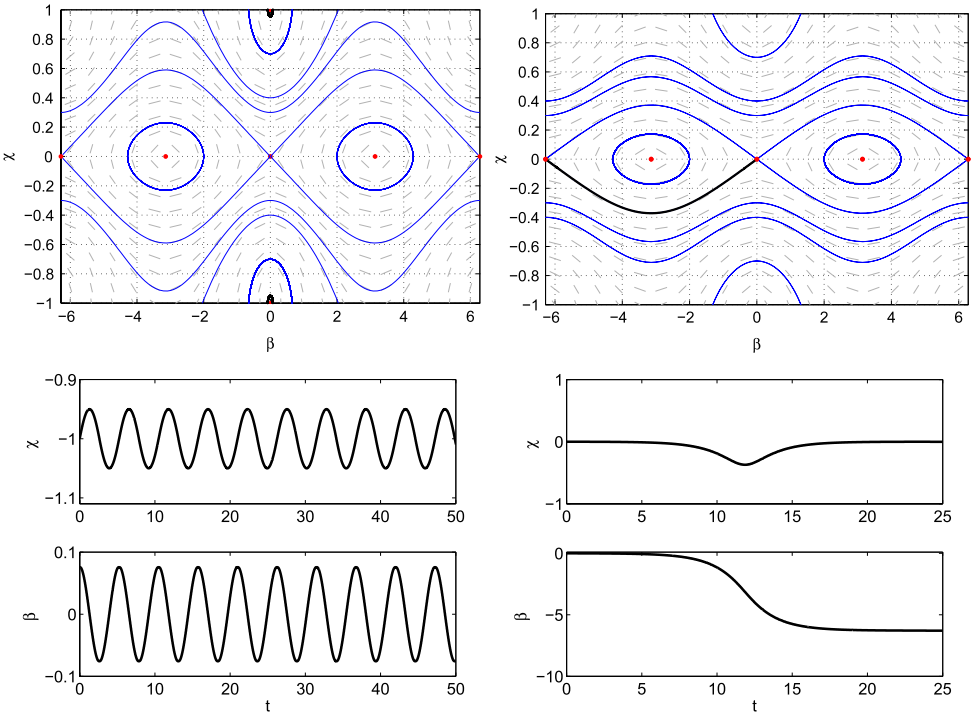

Fig. 4. Top left: phase portrait of the planar system (41) for $\epsilon = 0.1$ with $M = 1$, where the center point $(\beta_0, \chi_0) \approx (0, \pm 0.99)$ corresponds to the site-symmetric solution (32) and (33). Several trajectories are shown (solid lines) as well as the equilibrium points (solid circles). Bottom left: the time series of the trajectory with the initial value $(\beta, \chi) = (0, -0.95)$. Parts of the trajectory with $\chi < -1$ appear on the top part of the phase plane due to the 2-periodicity of χ, although in the time series plot we show them in the $\chi < -1$ region for clarity. Top right: phase portrait of the planar system (41) for $\epsilon = 0.1$ with $M = 1.79$, where the fixed point $(\beta_0, \chi_0) = (0, 0)$ corresponds to the bond-symmetric solution (31). Bottom right: the time series of the trajectory with the initial value $(\beta, \chi) = (0, -0.001)$, which is also shown in the top right panel (thicker line).

After M is defined by (43), we obtain

$$\lambda^2 = \frac{8\epsilon e^{-\eta}\sinh^3(\eta)}{\cosh^3(\eta)}(1+\sinh(\eta))(1-2e^{-\eta}) = 4\epsilon + \mathcal{O}(\epsilon^2). \tag{46}$$

Since $\lambda^2 > 0$ for small $\epsilon > 0$, we conclude that the bond-symmetric soliton approximated by Kaup's ansatz (10) with $s = \frac{1}{2}$ ($\chi = 0$) is unstable. This conclusion agrees with the result of spectral stability analysis in the DNLS equation [12]. Moreover, the asymptotic result $\lambda = 2\epsilon^{1/2} + \mathcal{O}(\epsilon^{3/2})$ is correctly recovered by the variational approximation (46). Fig. 5 shows the spectrum of the stability problem (4) linearized at the bond-symmetric solution for $\epsilon = 0.1$ (left) and the comparison between the variational and numerical approximations of the unstable eigenvalue as $\epsilon \to 0$ (right).

Near the critical point $(0, \chi_0)$, we find the perturbation equation $\ddot{\chi} + \omega^2(\chi - \chi_0) = 0$ with

$$\omega^2 = \frac{8\epsilon e^{-2\eta}\sinh^3(\eta)}{\cosh^3(\eta)}(\sinh(\eta)+\cosh(\eta\chi_0))\sinh^2(\eta\chi_0) = 2 + \mathcal{O}(\epsilon). \tag{47}$$

Since $\omega^2 > 0$ for small $\epsilon \in \mathbb{R}$, we conclude that the site-symmetric soliton approximated by Kaup's ansatz (10) with $s \approx 0$ ($\chi_0 \approx -1$) is stable. There are no small eigenvalues as $\epsilon \to 0$, but $\omega \approx \sqrt{2} + \mathcal{O}(\epsilon)$. This conclusion agrees again with the result of spectral stability analysis [12] but the variational eigenfrequency ω is not an accurate approximation of the purely imaginary eigenvalues of the spectral stability problem (4), which are known to be grouped into the band of the continuous spectrum near the point 1 [13]. Nevertheless, we show in the next section that it is the frequency $\omega \approx \sqrt{2} + \mathcal{O}(\epsilon)$ that occurs in the long-term oscillations of the site-symmetric soliton near the stable stationary solution.

4.2. Justification of the approximation based on ansatz $u^{(K)}$

To illustrate the accuracy of the time-dependent approximation (36), we compare its predictions with the time-dependent solutions of the DNLS equation (34), see Fig. 6. For periodic orbits near the stable center on the left panel of Fig. 4, we observe long-term oscillations of the error in time (left panel of Fig. 6). The oscillation amplitude is comparable with the initial error $\|u(0) - u^{(K)}(0)\|_{l^\infty} = 0.01$. For orbits near the unstable saddle on the right panel of Fig. 4, we observe a growth of the error in time (right panel of Fig. 6). As a result of instability, the bond-symmetric initial data with small initial error $\|u(0) - u^{(K)}(0)\|_{l^\infty} = 0.001$ transforms to the site-symmetric soliton, which correspond to the stable center point. Then, at a later time, recurrence phenomenon is observed and the solution of the DNLS equation (34) returns back to the nearly initial configuration.

We will now study the error of the variational approximation. The planar system (41) depends in a nontrivial way on the small parameter $\epsilon > 0$, which also determines η. However, as expansion (47) shows, the frequency at the stable critical point has the order of $\mathcal{O}(1)$ as $\epsilon \to 0$. Therefore, we can consider periodic trajectories of the planar system (41) in a neighborhood of the stable critical point which are located away from the heteroclinic trajectories. The following theorem gives the approximation result. For simplicity, we admit a convention that χ oscillates continuously near $\chi = -1$, as shown in the bottom left panel of Fig. 4, instead of assuming that χ is piecewise continuous due to the 2-periodic conditions on χ as shown in the top left panel of Fig. 4.

Theorem 6. *Fix $\epsilon_0 > 0$ and let $(\beta, \chi) \in C(\mathbb{R}, \mathbb{R}^2)$ be a family of periodic solutions of the planar system (41) such that for all $\epsilon \in (0, \epsilon_0)$, there exists $C_0 > 0$ such that*

$$\sup_{t\in\mathbb{R}} (|\beta(t)| + \eta|\chi(t) + 1|) \le C_0. \tag{48}$$

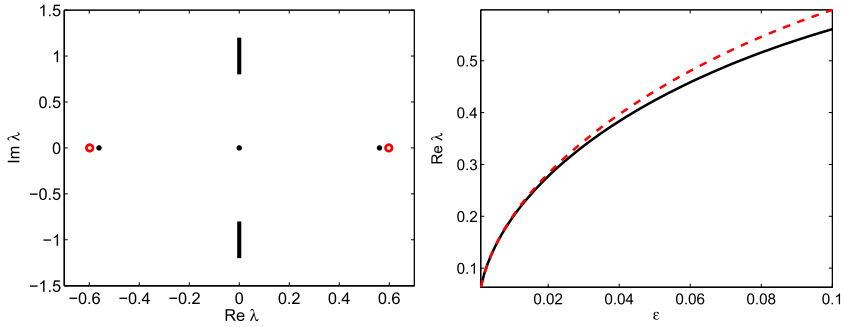

Fig. 5. Left: spectrum of the linearized operator for the bond-symmetric solution with $\epsilon = 0.1$. The solid markers represent numerically computed eigenvalues of the spectral stability problem (4) and the circles are given by the variational approximation (46). Right: unstable eigenvalue versus ϵ. The solid line shows the numerical computation and the dashed line shows the variational approximation (46).

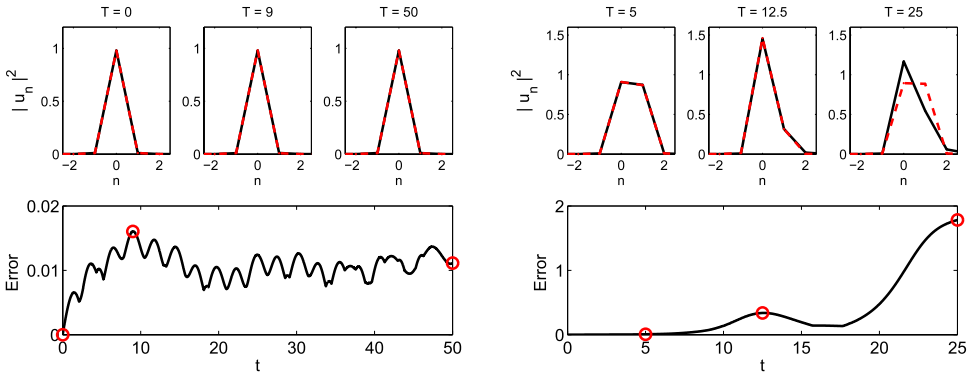

Fig. 6. Comparison between the variational approximation (36) and the numerical solutions of the DNLS equation (34), which correspond to the two computations in the bottom panels of Fig. 4. Left: evolution of the perturbed site-symmetric soliton. The top row shows the numerical solution (solid lines) and variational approximations (dashed lines) at three time instances. The bottom row is the error measured in the l^∞ norm versus time. The circles correspond to the time snap shots in the top row. Right: same as the left, but showing the evolution of the perturbed bond-symmetric soliton.

For all $\epsilon \in (0, \epsilon_0)$ and a given $T_0 > 0$, there exists T_0-dependent constant $C(T_0) > 0$ such that a time-dependent solution of the DNLS equation (34) with $u|_{t=0} = u^{(K)}|_{t=0}$ satisfies

$$\sup_{t\in[0,T_0]} \sup_{n\in\mathbb{Z}} |u_n(t) - u_n^{(K)}(t)| \le C(T_0)\epsilon. \tag{49}$$

Proof. We write a solution of the DNLS equation (34) as the sum of the variational approximation (36) and the error term,

$$u_n(t) = u_n^{(K)}(t) + U_n(t), \quad n \in \mathbb{Z}.$$

The error $U(t)$ satisfies

$$i\dot{U}_n = \mathcal{F}_n(U) + \mathrm{Res}_n(u^{(K)}), \tag{50}$$

where

$$\mathrm{Res}_n(u) = (1 - |u_n|^2)u_n - i\dot{u}_n - \epsilon(u_{n+1} + u_{n-1})$$

and

$$\begin{aligned}\mathcal{F}_n(U) = {} & (1 - 2|u_n^{(K)}|^2)U_n - (u_n^{(K)})^2\overline{U}_n - 2|U_n|^2u_n^{(K)} \\ & - U_n^2\overline{u}_n^{(K)} - |U_n|^2U_n - \epsilon(U_{n+1} + U_{n-1}).\end{aligned}$$

Evaluated at the trial function (36), the residual is given by,

$$\begin{aligned}\mathrm{Res}_n(u^{(K)}) = {} & Ae^{i\alpha+i\beta(n-s)-\eta|n-s|} \\ & \times \left[\dot{\alpha} + \dot{\beta}(n-s) - \beta\dot{s} - i\frac{\dot{A}}{A} - i\eta\,\dot{s}\,\mathrm{sign}(n-s)\right. \\ & + 1 - A^2e^{-2\eta|n-s|} - \epsilon\left(e^{i\beta-\eta|n+1-s|+\eta|n-s|}\right. \\ & \left.\left. + e^{-i\beta-\eta|n-1-s|+\eta|n-s|}\right)\right].\end{aligned}$$

Making use of Eqs. (38) and (39), we obtain

$$\begin{aligned}\mathrm{Res}_n(u^{(K)}) = {} & Ae^{i\alpha+i\beta(n-s)-\eta|n-s|} \\ & \times \left[-\frac{1}{2}\dot{\beta}\left(\frac{\tanh(\eta\chi)}{\tanh(\eta)} + 1 - 2n\right)\right. \\ & - \frac{i}{2}\eta\dot{\chi}\,(\mathrm{sign}(n-s) - \tanh(\eta\chi)) \\ & + 1 - A^2e^{-2\eta|n-s|} + H(\beta,\chi) \\ & \left. - \epsilon\left(e^{i\beta-\eta|n+1-s|+\eta|n-s|} + e^{-i\beta-\eta|n-1-s|+\eta|n-s|}\right)\right].\end{aligned}$$

The assumption (48) yields a bounded approximation $u^{(K)}(t)$ in the l^∞ norm. Since $l^\infty(\mathbb{Z})$ is a Banach algebra with respect to pointwise multiplication, for any ball B_δ of radius $\delta > 0$ in function space $C([0, T_0], l^\infty(\mathbb{Z}))$, there is δ-dependent constant $C_\delta > 0$ such that

$$\forall U \in B_\delta : \quad \|\mathcal{F}(U)\|_{l^\infty} \le C_\delta\|U\|_{l^\infty}. \tag{51}$$

Thanks to the global well-posedness of the DNLS equation [14], for any $T_0 > 0$, there exists a unique solution $U(t) \in C([0, T_0], l^2(\mathbb{Z}))$ of the inhomogeneous equation (50) with zero initial data $U(0) = 0$. We also recall the embedding of $l^2(\mathbb{Z})$ to $l^\infty(\mathbb{Z})$ such that $\|U\|_{l^\infty} \le \|U\|_{l^2}$.

It follows from (50) and (51) that for all small $\epsilon > 0$ and any given $T_0 > 0$, there is $C > 0$ such that

$$\begin{aligned}|U_n(t)| \le {} & |U_n(0)| + T_0\|\,\mathrm{Res}_n(u^{(K)})\|_{l^\infty} \\ & + C_\delta\int_0^{T_0}\|U(s)\|_{l^\infty}ds, \quad t \in [0, T_0],\end{aligned} \tag{52}$$

where $U(0) = 0$ is assumed initially. If we show that $\|\text{Res}(u^{(K)})\|_{l^\infty} = \mathcal{O}(\epsilon)$ as $\epsilon \to 0$, then a simple application of Gronwall's inequality yields the bound

$$\sup_{t\in[0,T_0]} \sup_{n\in\mathbb{Z}} |U_n(t)| \leq C(T_0)\epsilon,$$

which is nothing but the bound (49). Note that the constant $C(T_0)$ depends on T_0 and diverges as $T_0 \to \infty$.

To estimate the residual term, we note that the residual of the stationary variational approximation near the site-symmetric soliton with $(\beta, \chi) = (0, \chi_0)$ is largest at the site $n = -1$, where $R_{-1}(\psi^{(K)}) = \mathcal{O}(\epsilon^3)$. At this site, we compute the resolvent for the time-dependent variational approximation explicitly,

$$\begin{aligned}\text{Res}_{-1}(u^{(K)}) = Ae^{i\alpha - i\beta(3+\chi)/2 - \eta(3+\chi)/2}\Big[&1 - \cos(\beta) \\ &- A^2 e^{-\eta(3+\chi)} - 2\epsilon i \sin(\beta)\sinh(\eta) \\ &+ H(\beta,\chi) - \frac{1}{2}\dot\beta\left(\frac{\tanh(\eta\chi)}{\tanh(\eta)} + 3\right) \\ &+ \frac{i}{2}\eta\dot\chi\,(\tanh(\eta\chi) + 1)\Big]. \end{aligned} \tag{53}$$

We recall that the center point is $(\beta, \chi) = (0, \chi_0)$, where $\eta(\chi_0 + 1) = \mathcal{O}(\epsilon^2)$.

The expression for $H(\beta, \chi)$ from (40) can be rewritten in the equivalent form,

$$\begin{aligned} H(\beta,\chi) = &\frac{2e^{-4\eta}}{1+e^{-2\eta}} + \frac{\sinh(\eta)}{2\cosh(\eta)\cosh^2(\eta\chi)} \\ &\times \left(e^{-\eta(1+\chi)} - 1 + e^{-\eta(1-\chi)} + e^{-\eta(3+\chi)} + e^{-\eta(3-\chi)}\right) \\ &- 2\epsilon e^{-3\eta}\left(1 + \frac{\sinh(\eta)}{\cosh(\eta\chi)}\right) + 2\epsilon e^{-\eta}(\cos(\beta) - 1) \\ &\times \left(1 + \frac{\sinh(\eta)}{\cosh(\eta\chi)}\right). \end{aligned} \tag{54}$$

If (β, χ) satisfies the bound (48), then $|H(\beta, \chi)| = \mathcal{O}(\epsilon^2)$ and for any sufficiently small $\epsilon > 0$, there are ϵ-independent constants $C_1, C_2, C_3 > 0$ such that

$$|\text{Res}_{-1}(u^{(K)})| \leq \epsilon\left(C_1 + C_2|\dot\beta| + C_3|\eta\dot\chi|\epsilon^2\right). \tag{55}$$

The dynamical system (41) near the equilibrium point $(0, \chi_0)$ shows that $|\dot\beta| = \mathcal{O}(\eta(\chi - \chi_0))$ and $\eta|\dot\chi| = \mathcal{O}(\beta)$. Using these estimates and bounds (48) and (55), we obtain $\text{Res}_{-1}(u^{(K)}) = \mathcal{O}(\epsilon)$.

We shall now develop similar estimates for $n = 0$ and $n = 1$. Because of the discontinuity in the variable $\chi = 2s - 1$, when s is defined outside the main interval $s \in (0, 1)$, we should only consider the values of $s > 0$ for these calculations. Computations for $s < 0$ are similar. Using the explicit formula, we obtain

$$\begin{aligned}\text{Res}_0(u^{(K)}) = Ae^{i\alpha - i\beta(1+\chi)/2 - \eta(1+\chi)/2}\Big[&1 - A^2 e^{-\eta(1+\chi)} - \epsilon e^{-\eta}(e^{i\beta+\eta(1+\chi)} + e^{-i\beta}) \\ &+ H(\beta,\chi) - \frac{1}{2}\dot\beta\left(\frac{\tanh(\eta\chi)}{\tanh(\eta)} + 1\right) \\ &+ \frac{i}{2}\eta\dot\chi\,(\tanh(\eta\chi) + 1)\Big]. \end{aligned}$$

Since $M = 1$, we have

$$1 - A^2 e^{-\eta(1+\chi)} = e^{-2\eta}\frac{1 + e^{2\eta(1+\chi)}}{1 + e^{2\eta\chi}} = \mathcal{O}(\epsilon^2),$$

$$\frac{\tanh(\eta\chi)}{\tanh(\eta)} + 1 = -2e^{-2\eta}\frac{1 - e^{2\eta(1+\chi)}}{(1 - e^{-2\eta})(1 + e^{2\eta\chi})} = \mathcal{O}(\epsilon^2),$$

and

$$\tanh(\eta\chi) + 1 = 2e^{-2\eta}\frac{e^{2\eta(1+\chi)}}{1 + e^{2\eta\chi}} = \mathcal{O}(\epsilon^2).$$

Therefore, under the condition (48), we obtain $\text{Res}_0(u^{(K)}) = \mathcal{O}(\epsilon^2)$.

Using the explicit formula again, we obtain

$$\begin{aligned}\text{Res}_1(u^{(K)}) = Ae^{i\alpha + i\beta(1-\chi)/2 - \eta(1-\chi)/2}\Big[&1 - A^2 e^{-\eta(1-\chi)} - \epsilon(e^{i\beta-\eta} + e^{-i\beta-\eta\chi}) \\ &+ H(\beta,\chi) - \frac{1}{2}\dot\beta\left(\frac{\tanh(\eta\chi)}{\tanh(\eta)} - 1\right) \\ &+ \frac{i}{2}\eta\dot\chi\,(\tanh(\eta\chi) - 1)\Big], \end{aligned}$$

which satisfies the bound (55) yielding $\text{Res}_1(u^{(K)}) = \mathcal{O}(\epsilon)$.

Developing similar estimates for $|n| \geq 2$, we obtain $\|\text{Res}(u^{(K)})\|_{l^\infty} = \mathcal{O}(\epsilon)$, which yields the result of the theorem. □

Corollary 7. *Under the conditions of Theorem 6, if $(\beta, \chi) \in C(\mathbb{R}, \mathbb{R}^2)$ satisfies*

$$\sup_{t\in\mathbb{R}}(|\beta(t)| + \eta|\chi(t) + 1|) \leq C_0\epsilon^2, \tag{56}$$

which coincides with the scaling of the center point $(\beta, \chi) = (0, \chi_0)$, then the variational approximation satisfies the bound

$$\sup_{t\in[0,T_0]} \sup_{n\in\mathbb{Z}} |u_n(t) - u_n^{(K)}(t)| \leq C(T_0)\epsilon^3, \tag{57}$$

or equivalently,

$$\sup_{t\in[0,T_0\epsilon^{-2}]} \sup_{n\in\mathbb{Z}} |u_n(t) - u_n^{(K)}(t)| \leq C(T_0)\epsilon, \tag{58}$$

which are better approximations compared to (49).

Proof. Under condition (56), we obtain from (53) and (54) that $|H(\beta, \chi)| = \mathcal{O}(\epsilon^4)$ and

$$|\text{Res}_{-1}(u^{(K)})| \leq \epsilon\left(C_0\epsilon^2 + C_1|\beta|^2 + C_2|\dot\beta| + C_3|\eta\dot\chi|\epsilon^2\right) = \mathcal{O}(\epsilon^3).$$

Similarly, $|\text{Res}_0(u^{(K)})| = \mathcal{O}(\epsilon^4)$ and $|\text{Res}_1(u^{(K)})| = \mathcal{O}(\epsilon^3)$, and the result of Corollary 7 follows by the Gronwall inequality from the estimate (52) with $\|\text{Res}(u^{(K)})\|_{l^\infty} = \mathcal{O}(\epsilon^3)$ as $\epsilon \to 0$. □

The results of Theorem 6 and Corollary 7 are shown in Fig. 7 by comparing the variational approximations and the numerical solutions of the time-dependent DNLS equation (34) for various values of ϵ with $T_0 = 50$.

5. Conclusion

We have provided a general framework to justify the use of the variational approximation in discrete nonlinear Schrödinger equations in the limit of small coupling. We have discovered that the trial function for the stationary discrete solitons with more parameters provides more accurate approximations, which have the error converging to zero as $\epsilon \to 0$ with a higher exponent in ϵ. Adding more parameters to the trial functions can be used both to improve variational approximations to the site-symmetric and bond-symmetric solitons and to approximate other families of multi-site discrete solitons.

We also studied errors of the time-dependent Kaup's approximation that interpolates between site-symmetric and bond-symmetric discrete solitons. We found that the error of the time-dependent variational approximation is generally larger than that of the stationary approximation as a function of ϵ but it is still kept small for finite but large time intervals. If the periodic solutions are defined in the neighborhood of the center point on

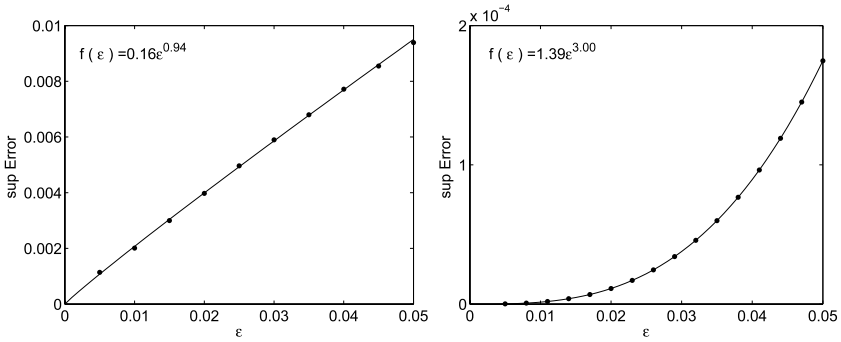

Fig. 7. Left: error of the time-dependent variational approximation (36) and the numerical solution of the DNLS equation (34) measured with $\sup_{t\in[0,T_0]}\|u(t)-u^{(K)}(t)\|_{l^\infty}$ for periodic solution of system (41) satisfying (48). The solid line $f(\epsilon)=0.16\epsilon^{0.94}$ represents the best power fit. Right: same as left, but for periodic solutions satisfying (56) and with $f(\epsilon)=1.39\epsilon^{3.00}$.

the effective phase plane, the error can be kept as small as that for the stationary variational approximation or can be extended to remain small for longer time intervals.

As a particular interest, we note that the frequency of oscillations near the center point $\left(\approx\sqrt{2}\right)$ does not coincide with the frequency of oscillations of linear perturbations of the discrete solitons ($\approx$ 1) and it is the former frequency that is observed in our numerical simulations and in the rigorous justification (Theorem 6). This can be understood that the frequency $\left(\approx\sqrt{2}\right)$ represents coherent dynamics of a discrete soliton whereas the frequency ($\approx$ 1) represents dynamics of nearly harmonic oscillators at the lattice sites far from the discrete soliton.

We expect that similar results can be obtained for other variants of DNLS equations, such as those with higher order nonlinearities [6,15] or ones with extended linear coupling [16,17], although an ansatz with more than the four parameters considered here would probably be needed due to the complex dynamics occurring in such models. It would also be interesting to explore the validity of the VA in higher dimensional lattices.

Acknowledgments

The work of C. Chong and G. Schneider is partially supported by the Deutsche Forschungsgemeinschaft (DFG) grant SCHN 520/8-1. The work of D. Pelinovsky is partially supported by the Humboldt Research Foundation.

References

[1] P.G. Kevrekidis, The Discrete Nonlinear Schrödinger Equation: Mathematical Analysis, Numerical Computations and Physical Perspectives, Springer, New York, 2009.
[2] D.E. Pelinovsky, Localization in Periodic Potentials: From Schrödinger Operators to the Gross–Pitaevskii Equation, Cambridge University Press, Cambridge, 2011.
[3] D.J. Kaup, B.A. Malomed, Embedded solitons in lagrangian and semi-lagrangian systems, Physica D 184 (2003) 153–161.
[4] B.A. Malomed, Variational methods in nonlinear fiber optics and related fields, Progr. Opt. 43 (2002) 71–193.
[5] D.J. Kaup, T.K. Vogel, Quantitative measurement of variational approximations, Phys. Lett. A 362 (2007) 289–297.
[6] C. Chong, D.E. Pelinovsky, Variational approximations of bifurcations of asymmetric solitons in cubic-quintic nonlinear Schrödinger lattices, DCDS-S 4 (2011) 1019–1032.
[7] J. Cuevas, G. James, P.G. Kevrekidis, B.A. Malomed, B. Sánchez-Rey, Approximation of solitons in the discrete NLS equation, J. Nonlinear Math. Phys. 15 (2008) 124–136.
[8] D.J. Kaup, Variational solutions for the discrete nonlinear Schrödinger equation, Math. Comput. Simulation 69 (2005) 322–333.
[9] H. Susanto, P.C. Matthews, Variational approximations to homoclinic snaking, Phys. Rev. E 83 (2011) 035201(R).
[10] B.A. Malomed, M.I. Weinstein, Soliton dynamics in the discrete nonlinear Schrödinger equation, Phys. Lett. A 220 (1996) 91–96.
[11] J. Cuevas, P.G. Kevrekidis, D.J. Frantzeskakis, B.A. Malomed, Discrete solitons in nonlinear Schrödinger lattices with a power-law nonlinearity, Physica D 238 (2009) 67–76.
[12] D.E. Pelinovsky, P.G. Kevrekidis, D. Frantzeskakis, Stability of discrete solitons in nonlinear Schrödinger lattices, Physica D 212 (2005) 1–19.
[13] D. Pelinovsky, A. Sakovich, Internal modes of discrete solitons near the anti-continuum limit of the dNLS equation, Physica D 240 (2011) 265–281.
[14] G.M. N'Guerekata, A. Pankov, Global well-posedness for discrete nonlinear Schrödinger equation, Appl. Anal. 89 (2010) 1513–1521.
[15] R. Carretero-González, J.D. Talley, C. Chong, B.A. Malomed, Multistable solitons in the cubic-quintic discrete nonlinear Schrödinger equation, Physica D 216 (2006) 77–89.
[16] C. Chong, R. Carretero-González, B.A. Malomed, P.G. Kevrekidis, Variational approximations in discrete nonlinear Schrödinger equations with next-nearest-neighbor couplings, Physica D 240 (2011) 1205–1212.
[17] K.Ø. Rasmussen, P.L. Christiansen, Y.B. Johansson, M. Gaididei, S.F. Mingaleev, Localized excitations in discrete nonlinear Schrödinger systems: effects of nonlocal dispersive interactions and noise, Physica D 113 (1998) 134–151.